IS-M 855
CONF-960796--5
Abstract Number: IY-02

NEUTRON AND RESONANT X-RAY SCATTERING STUDIES OF RNi_2B_2C (R=rare earth) SINGLE CRYSTALS

C. Stassis and A. I. Goldman

Ames Laboratory, and Dept. of Physics and Astronomy, Iowa State University, Ames, Iowa 50011, U.S.A.

Abstract

This family of intermetallic compounds is ideal for the study of the interplay between superconductivity and magnetism since, in several of these compounds (Ho, Er, Tm, Dy), superconductivity coexists with magnetic ordering. The most important findings of our scattering studies are (a) in the Ho-compound, a complex magnetic structure characterized by two incommensurate wave vectors, $\vec{k}_a = 0.585\ \vec{a}^*$ and $\vec{k}_c = 0.915\ \vec{c}^*$, exists in the vicinity of 5 K, where the almost reentrant behavior of this compound occurs (below 4.7 K, it is a commensurate antiferromagnet); (b) an incommensurate magnetic structure with wave vector along $\vec{a}^*$, close to the zone boundary, is observed in several of these compounds (Ho, Er, Tb, Gd); and (c) pronounced soft-phonon behavior was observed for both the acoustic and first optical $\Delta_4[\xi 00]$ branches in the superconducting Lu and Ho compounds, a behavior characteristic of strongly coupled conventional superconductors. Furthermore, these phonon anomalies occur at wave vectors close to those of the incommensurate magnetically ordered structures observed in the magnetic compounds of this family (see (b)). This observation suggests that both the magnetic ordering and phonon softening originate from common

DISCLAIMER

nesting features of the Fermi surfaces of these compounds. Band theoretical calculations are in qualitative agreement with these results.

I. Introduction

The low temperature physical properties of the recently discovered (1-4) family of rare-earth nickel boride carbides, RNi_2B_2C (where R stands for a rare-earth element), have been the subject of many theoretical and experimental investigations. The structure (3) of these compounds is body-centered tetragonal (space group I4/mmm) and consists of R-C layers separated by Ni_2B_2 sheets (Fig. 1); typically a $\cong$3.5 Å and c$\cong$3a. The interest in these compounds is due to the diversity of their magnetic and superconducting properties. Many of these compounds (Lu, Y, Tm, Er, Ho, Dy) are superconducting, and the highest superconducting temperatures observed (2-5) are 16.6 K for the Lu, and 15.6 K for the Y compound.

It is particularly interesting that superconductivity is observed not only in compounds containing non-magnetic rare-earth elements, for instance Lu and Y, but also in compounds containing magnetic rare-earth elements such as Tm, Er, Ho, and Dy (2-7) with superconducting transition temperatures, T_c, of 10.8, 10.5, 8.7, and 6.2 K, respectively. In the Tm, Ho, and Er compounds the magnetic ordering temperature, T_N, is below T_c, whereas in the Dy compound $T_N > T_c$. Many other members of this family formed with magnetic rare-earth elements (Gd, Tb, Nd, Sm) order magnetically at low temperatures, but are not superconducting at least down to approximately 2 K. Some of the properties of these compounds are summarized in Table I.

It is clear from this brief survey of their properties that these compounds are particularly well suited to a detailed study of the subtle interplay between superconductivity and magnetism. For instance, the relatively high superconducting and magnetic transition temperatures of these compounds make their study easier, from the experimental point of view, than that of the previously examined (8-11) RRh_4B_4 and RMo_6S_8 families of magnetic superconductors.

Relatively large single crystals of these compounds were first grown (12) at the Ames Laboratory and this made possible the systematic study of their properties. The results of magnetization and resistivity measurements are outlined in the paper by P. Canfield (13). In the present paper, we present the results, obtained by neutron scattering and resonant x-ray scattering techniques, of the magnetic structure and the lattice dynamics of these compounds.

II. Experimental Details

The samples used in the present experiments were single crystals of high perfection (measured full width at half maximum $\cong 0.1°$) depleted in the strongly absorbing B^{10} nuclei for the neutron measurements. Since the size of the crystals (approximately $5\times5\times0.5$ mm^3) is relatively small for inelastic neutron scattering experiments, a composite crystal consisting of two of these crystals was used for the lattice dynamical studies; the two crystals were mounted together and their alignment was adjusted until their Bragg reflections were found to coincide to within the instrumental resolution.

Both the magnetic structure and lattice dynamics of these compounds were studied by making use of triple-axis spectrometers at the HFIR reactor of the Oak Ridge National Laboratory and HFBR reactor of the Brookhaven National Laboratory. Pyrolitic graphite, reflecting from the (002) planes, was used as both monochromator and analyzer. Most measurements were performed with a constant-scattered-neutron energy (14.7 meV) and a pyrolytic graphite filter was used to attenuate higher-order contaminations. Typically, the collimation before the sample was either 20 or 40 minutes of arc and that after the sample was 40 minutes of arc.

Resonant x-ray scattering studies of the heavily neutron absorbing Gd and Sm members of this family were performed at the Brookhaven X22C beamline at the National Synchrotron Light Source. The technique itself has been described elsewhere (14). Here we point out that the technique utilizes atomic absorption edges to obtain large enhancements of the scattering cross-section at magnetic Bragg peaks. For the cases at hand, most work was done at the Gd and Sm L_2 absorption edges.

III. Magnetic Structure

As expected from the crystal structure of these compounds, only nuclear reflections with $h+k+\ell = 2n$ are observed above the magnetic transition temperature, T_N, of these compounds. Below T_N magnetic diffraction peaks start developing in rows parallel to some direction of the reciprocal lattice, which can be indexed as first- and higher-order satellites of the allowed ($h+k+\ell = 2n$) nuclear reflections; the direction of the rows

determines the direction of the propagation vector. Since the neutron scattering cross-section depends only on the component of the moment perpendicular to the neutron scattering vector, the intensities of the observed magnetic peaks can be used to determine the direction and magnitude of the ordered moments. Similarly, the angular dependence of the resonant x-ray scattering can be used to determine the moment direction (15).

Commensurate Magnetic Structures

In Dy (T_c = 6.2 K), below approximately 10 K, magnetic scattering develops (7) at the positions of the forbidden nuclear reflections (hkℓ) with h+k+ℓ = 2n+1 as it can be seen in the scan along c* taken at 5 K (Fig. 2). As the temperature decreases below 10 K the intensities of the magnetic reflections increase and start to saturate below approximately 8 K. Thus, below approximately 10 K, the Dy compound is a commensurate antiferromagnet. In this temperature range, the moments are aligned ferromagnetically in each layer perpendicular to the c-axis with the magnetic moments of two consecutive layers aligned in opposite direction. The same simple commensurate antiferromagnetic structure was observed (16-17) in $HoNi_2B_2C$ (T_c = 8 K) at temperatures below 4.7 K. A different commensurate antiferromagnetic structure, with propagation vector along the [101] direction, was also observed by magnetic x-ray scattering techniques (18) in the non-superconducting Sm compound and by neutron measurements in the Nd compound (19).

Incommensurate Magnetic Structures

Of particular interest are the incommensurate magnetic structures observed in the ordered state of many of these compounds. In Er(T_c = 10.5 K), below approximately 7 K, magnetic diffraction peaks appear (20-21) in rows parallel to the reciprocal a-axis (or the equivalent b-axis of the tetragonal structure) (Fig. 3). These peaks can be indexed as first and higher-order satellites of the allowed nuclear reflections with an incommensurate wave vector (0.553 0 0). The modulation is transverse with a propagation vector of 0.553 along $\vec{a}^*$ (or $\vec{b}^*$), and the observation of higher-order harmonics shows that the modulation is not purely sinusoidal but squared. A similar structure with wave vector (0.585 0 0) was also observed (12,22) in the Ho compound between approximately 6 K and 4.7 K. In the Ho compound, however, an additional incommensurate modulation of wave vector of 0.915 along c* was observed (16-17) between 6 K and 4.7 K. Since this complex two-component incommensurate magnetic structure occurs in the vicinity of 5 K, it is reasonable to assume that the almost reentrant behavior of this compound at 5 K is due to the pair-breaking interactions associated with this modulated structure.

An incommensurate modulation of the moments with propagation vector along $\vec{a}^*$ was also observed (23) in the Tb compound which is not superconducting at least down to 2 K. The magnetic transition temperature is approximately 15 K and the magnitude of the propagation vector changes from 0.51 at 15 K to 0.545 at 2.3 K, the lowest temperature reached in the experiments. The magnetic structure of the Tb compound is, however, quite

different from that of the Er compound. In Tb (see Fig. 4), the intensities of the (h00) satellites are considerably lower than those of the corresponding (h0 ℓ) satellites. Since, as we mentioned earlier, the neutron senses only the component of the magnetic moment perpendicular to the scattering vector, this implies that the direction of the moments is close to that of the $\vec{a}^*$-axis; the moments order in an almost longitudinal wave with wave vector along $\vec{a}^*$. A modulated incommensurate magnetic structure with a wave vector of 0.553 along $\vec{a}^*$ was also observed (24) in the non-superconducting Gd compound below T_N = 19 K by magnetic x-ray scattering techniques. The wave vector of the modulation, as in the case of Tb, also evolves with temperature. Further, for the Gd compound there is a second magnetic transition below approximately 14 K. Between 14 K and 19 K the magnetic structure is identical to that found in $ErNi_2B_2C$. Below 14 K, a component of the moment along the c-axis develops.

It is interesting that an incommensurate magnetic structure with wave vector along $\vec{a}^*$ is a common feature of the magnetic structures of several of these compounds (Ho,Er,Tb,Gd). The magnitude of the wave vector does not vary appreciably among these compounds and it is close to that of the zone boundary point G_1 along $\vec{a}^*$. These results suggest that there are common nesting features along $\vec{a}^*$in the RNi_2B_2C family that cause the ordering of the rare-earth moment via the RKKY mechanism. This is in qualitative agreement with the results of band theoretical calculations (25) of the generalized electronic susceptibility, $\chi(q)$, of $LuNi_2B_2C$ based on the normal-

state electronic band structure of this compound. The calculated electronic susceptibility along $\vec{a}^*$ exhibits a strong peak, due to Fermi surface nesting, at a wave vector of magnitude close to that observed in Ho, Er, Tb, and Gd compounds.

IV. Phonon Dispersion Curves

Electronic band structure calculations (26-29) suggest that the superconducting members of these compounds are conventional superconductors with a rather complex set of bands, crossing E_F, strongly coupled to the phonons. In addition, if a strong Fermi surface nesting is indeed present (see III), one also would expect to find Kohn anomalies in the phonon dispersion curves of these compounds close to the zone boundary point, G_1, along the [ξ00] direction. This motivated the study of the dispersion curves of these compounds.

The phonon dispersion curves of Lu and Ho were studied (30-31) by standard inelastic neutron scattering techniques. Because of the relatively small size of the presently available crystals (see II) only the low energy (< 40 meV) branches were measured. The most interesting result of these experiments is the temperature dependence of the phonon frequencies of the lowest lying acoustic and optical branches along the [ξ00] direction. By symmetry, the acoustic branch belongs to the Δ_4 representation. The lowest lying optical branch in this direction was also assigned to the Δ_4 representation on the basis of a Born-von Kármán model analysis of the

experimental data. For small wave vectors both Δ_4 branches are purely transverse with atomic displacements along the c-axis. For the acoustic branch all atoms move in phase, whereas for the optical branch the motion of the rare-earth atoms is out of phase with that of the other atoms. For larger values of the wave vector, the rare earth and C displacements remain transverse, while the Ni and B atoms develop a longitudinal component.

The results obtained for the temperature dependence of these two branches are plotted in Fig. 5. It can be seen that the frequencies of the acoustic and first optical Δ_4 branches decrease with decreasing temperature and, at low temperatures, exhibit pronounced dips close to the zone-boundary point G_1.

The observation of strong phonon softening shows that the electron phonon interaction is quite strong in the Lu and Ho compounds resulting in incipient lattice instability. Such a behavior is typical of strongly coupled conventional superconductors. This observation provides experimental support for the arguments based on band theoretical calculations (26-29) that $LuNi_2B_2C$ is a conventional superconductor.

It is also important to notice that the softening occurs at a wave vector close to that of the zone-boundary point G_1. This value is close to the values of the incommensurate magnetic wave vector along $\vec{a}^*$observed in Ho, Er, Tb, and Gd and in quite good agreement with the value of the Fermi surface nesting wave vector obtained by band theoretical calculations (25) of the generalized electronic susceptibility. Therefore, it is tempting to argue that in

some of the magnetic compounds of this family, due to the nesting of the Fermi surface, phonon softening and magnetic ordering are competing to decrease the energy of the system.

V. Summary

A large variety of magnetic structures, ranging in complexity from the commensurate antiferromagnetic structure observed in several compounds to the two-component incommensurate structure observed is Ho between 4.7 and 6 K, have been observed in the compounds of the RNi_2B_2C family by neutron and resonant x-ray scattering techniques. Of particular interest is the two-component incommensurate structure of Ho, since the pair-breaking mechanism associated with this structure may be responsible for the almost reentrant behavior of this compound in the vicinity of 5 K. Certainly, theoretical calculations assessing the importance of the pair-breaking mechanism associated with incommensurate modulations may contribute to our understanding of the properties of the magnetic superconductors of this interesting family.

The observations of strong temperature-dependent phonon anomalies in the dispersion curves of the Lu and Ho compounds shows that these compounds are strongly coupled conventional superconductors. Since the phonon anomalies occur at wave vectors close to those of the incommensurate magnetic structure observed in several members of this family (Ho,Er,Gd,Tb), it is tempting to assume that both the magnetic ordering and the incipient lattice instabilities are strongly influenced by

common nesting features of the Fermi surfaces of the RNi_2B_2C compounds. This observation is supported by the results of band theoretical calculations of the generalized electronic susceptibility of the Lu compound.

References

1. R. Nagarajan, C. Mazumdar, Z. Hossain, S. K. Dhar, K V. Gopalakrishnan, L. C. Gupta, C. Godart B. D. Padalia, and R. Vijayaraghavan, *Phys. Rev. Lett.* **72**, 274 (1994).
2. R. J. Cava, H. Takagi, H. W. Zandbergen, J. J. Krajewski, W. F. Peck, Jr., T. Siegrist, B. Batlogg, R. B. van Dover, R. J. Felder, K. Mizuhashi, J. O. Lee, H. Eisaki, and S. Uchida, *Nature* **367**, 252 (1994).
3. T. Siegrist, H. W. Zandbergen, R. J. Cava. J. J. Krajewski, and W. F. Peck, Jr., *Nature* **367**, 254 (1994).
4. R. Cava, H. Takagi, B. Batlogg, H. W. Zandbergen, J. J. Krajewski, W. F. Peck, Jr., R. B. van Dover, R. J. Felder, T. Siegrist, K. Mizuhashi, J. O. Lee, H. Eisaki, S. A. Cater, and S. Uchida, *Nature* **367**, 146 (1994).
5. H. Eisaki, H. Takagi, R. J. Cava, K. Mizuhashi, J. O. Lee, B. Batlogg, J. J. Krajewski, W. F. Peck, Jr., and S. Uchida, *Phys. Rev. B* **50**, 647 (1994).
6. B. K. Cho, P. C. Canfield, and D. C. Johnston, *Phys. Rev. B* **52**, R3844 (1995).
7. P. Dervenagas, J. Zarestky, C. Stassis, A. I. Goldman, P. C. Canfield, B. K. Cho, *Physica B* **212**, 1 (1995).
8. *Proceedings of the International Conference on Ternary Superconductors*, edited by G. K. Shenoy, B. D. Dunlap, and F. Y. Fradin (North-Holland, Amsterdam, 1981).

9. *Superconductivity in Ternary* Compounds, Vols. I and II of *Topics in Current Physics*, edited by M. B. Maple and O. Fischer (Springer, Berlin, 1982).

10. S. K. Sinha. G. W. Crabtree, D. G. Hinks, and H. A. Mook, *Phys. Rev. Lett.* **48**, 950 (1982).

11. S. K. Sinha, H. A. Mook, O. A. Pringle, D. G. Hinks, in *Superconductivity in Magnetic and Exotic Materials*; Proceedings of the 6th Taniguchi International Symposium, Kashikojima, Japan, 1983, edited by T. Matsubara and A. Kotani, Springer Series in Solid-State Sciences, Vol. 52 (Springer-Verlag, New York, 1984) pp. 14-28.

12. M. Xu, P. C. Canfield, J. E. Ostenson, D. K. Finnemore, B. K. Cho, Z. R. Wang, and D. C. Johnston, *Physica C* **227**, 321 (1994).

13. P. C. Canfield, this volume

14. D. Gibbs, G. Grübel, D. R. Harshmans, E. D. Isaacs, D. B. McWhon, D. Mills, and C. Vettler, *Phys. Rev. B* **43**, 5663.

15. J. P. Hill and D. F. McMorrow, *Acta Crystal.* A **52**, 236 (1996).

16. A. I. Goldman, C. Stassis. P. C. Canfield, J. Zarestky, P. Dervenagas, B. K. Cho, D. C. Johnston, and B. Sternlieb, *Phys. Rev. B* **50**, 9668 (1995).

17. T. E. Grigereit, J. W. Lynn, Q. Huang, A. Santoro, R. J. Cava, J. J. Krajewski, W. F. Peck, Jr., *Phys. Rev. Lett.* **73**, 2756 (1994).

18. C. Detlefs et al., (unpublished).

19. A. I. Goldman et al., (unpublished).

20. J. Zarestky, C. Stassis, A. I. Goldman, P. C. Canfield, P. Dervenagas, B. K. Cho, and D. C. Johnston, *Phys. Rev. B* **51**, 678 (1995).

21. S. K. Sinha, J. W. Lynn, T. E. Grigereit, Z. Hossain, L. C. Gupta, R. Nagarajan, and C. Godart, *Phys. Rev. B* **51**, 681 (1995).

22. T. Vogt, A. Goldman, B. Sternlieb, and C. Stassis,*Phys. Rev. Lett.* **75**, 2628 (1995).

23. P. Dervenagas, J. Zarestky, C. Stassis, A. I. Goldman, P. C. Canfield, B. K. Cho, *Phys. Rev. B* (in press).

24. C. Detlefs, A. I. Goldman, C. Stassis, P. Canfield, B. K. Cho, J. P. Hill, D. Gibbs, *Phys. Rev. B* **53**, 6355 (1996).

25. J. Y. Rhee, X. Wang, and B. N. Harmon, *Phys. Rev. B* **51**, 15,585 (1995). Inadvertently, incorrect k_z values for the Fermi surface cross-sections were listed in this reference. The correct k_z values are 0.0, 0.2, 0.35, and 0.45 in units of $2\pi/c$.

26. W. E. Pickett and D. J. Singh, *Phys. Rev. Lett.* **72**, 3702 (1994).

27. L. F. Mattheiss, *Phys. Rev. B* **49**, 13,279 (1994).

28. R. Coehoorn, *Physica C* **228**, 5671 (1994).

29. L. F. Mattheiss, T. Siegrist, and R. J. Cava, *Solis State commun.* **91**, 587 (1994).

30. P. Dervenagas, M. Bullock, J. Zarestky, P. Canfield, B. K. Cho, B. Harmon, A. I. Goldman, C. Stassis *Phys. Rev. B* **52**, 9839 (1995).

31. M. Bullock et al. (to be published).

Figure Captions

Fig. 1. Crystal structure of the RNi_2B_2C compounds.

Fig. 2. Typical neutron diffraction scans (7) along $\vec{c}^*$, at 19 and 5 K. Four monitors correspond to a counting interval of approximately 3.6 sec.

Fig. 3. Neutron diffraction scan (20) along the $\vec{a}^*$ direction. One monitor corresponds to a counting interval of approximately 1 sec.

Fig. 4. Typical scans (23) along the [h01] and [h00] symmetry directions. The satellites of a (h0 ℓ) reflection are denoted by $(h0\,\ell)_n^{\pm}$ where the superscript + (or -) means that the magnetic wave vector is added (or subtracted) from the reciprocal vector of the reflection, and the subscript n is the order of the satellite.

Fig. 5. The $\Delta_4[\xi 00]$ branches (30) at 295 and 10 K. The lines through the 10 K points are intended as guides to the eye.

Table I. Superconducting and magnetic ordering temperatures of some RNi_2B_2C compounds

R	T_c (K)	T_N(K)
Y	15.6	--
Lu	16.6	--
Tm	10.8	1.5
Er	10.5	7
Ho	8.7	6
Dy	6.2	10
Tb	--	15
Gd	--	19
Sm	--	9
Nd	--	5

Table I. Superconducting and magnetic ordering temperatures of some RNi_2B_2C compounds

R	T_c (K)	T_N(K)
Y	15.6	--
Lu	16.6	--
Tm	10.8	1.5
Er	10.5	7
Ho	8.7	6
Dy	6.2	10
Tb	--	15
Gd	--	19
Sm	--	9
Nd	--	4.5

Figure Captions

Fig. 1. Crystal structure of the RNi_2B_2C compounds.

Fig. 2. Typical neutron diffraction scans (7) along $\vec{c}^*$, at 19 and 5 K. Four monitors correspond to a counting interval of approximately 3.6 sec.

Fig. 3. Neutron diffraction scan (20) along the $\vec{a}^*$ direction. One monitor corresponds to a counting interval of approximately 1 sec.

Fig. 4. Typical scans (23) along the [h01] and [h00] symmetry directions. The satellites of a (h0 ℓ) reflection are denoted by $(h0\,\ell)_n^{\pm}$ where the superscript + (or -) means that the magnetic wave vector is added (or subtracted) from the reciprocal vector of the reflection, and the subscript n is the order of the satellite.

Fig. 5. The $\Delta_4[\xi 00]$ branches (30) at 295 and 10 K. The lines through the 10 K points are intended as guides to the eye.

$Re\ Ni_2\ B_2\ C$

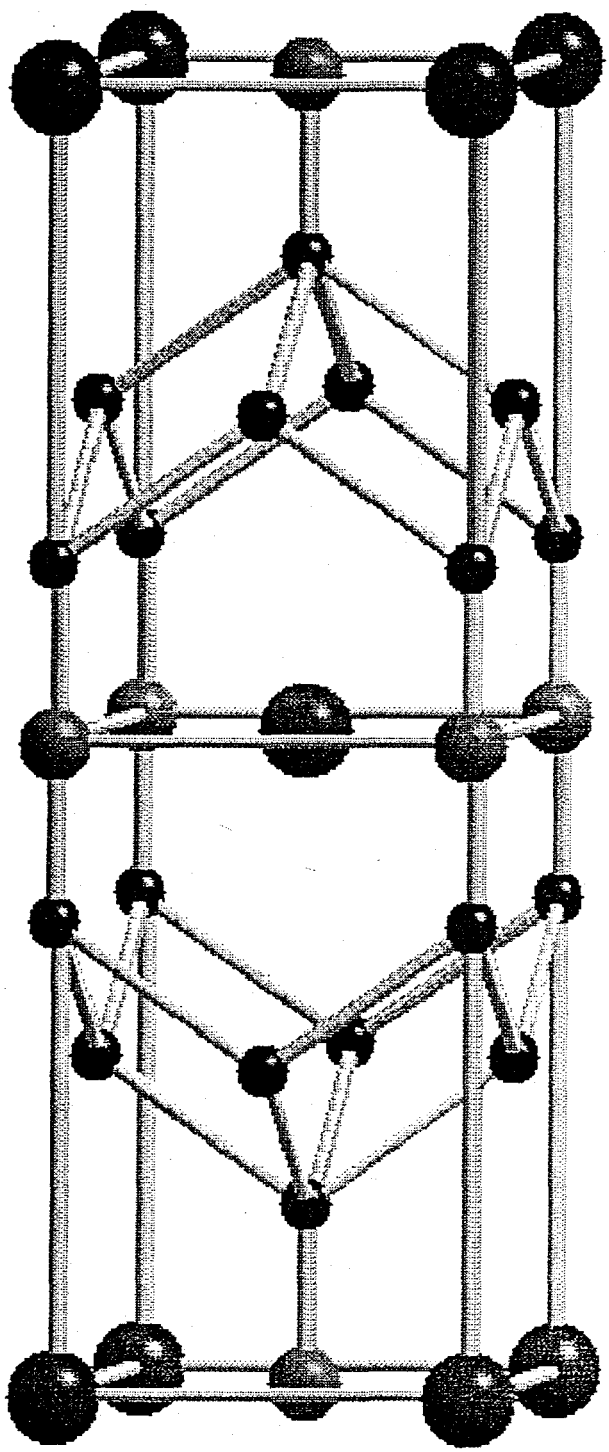

Re -Red
C -Grey
Ni -Blue
B -Green

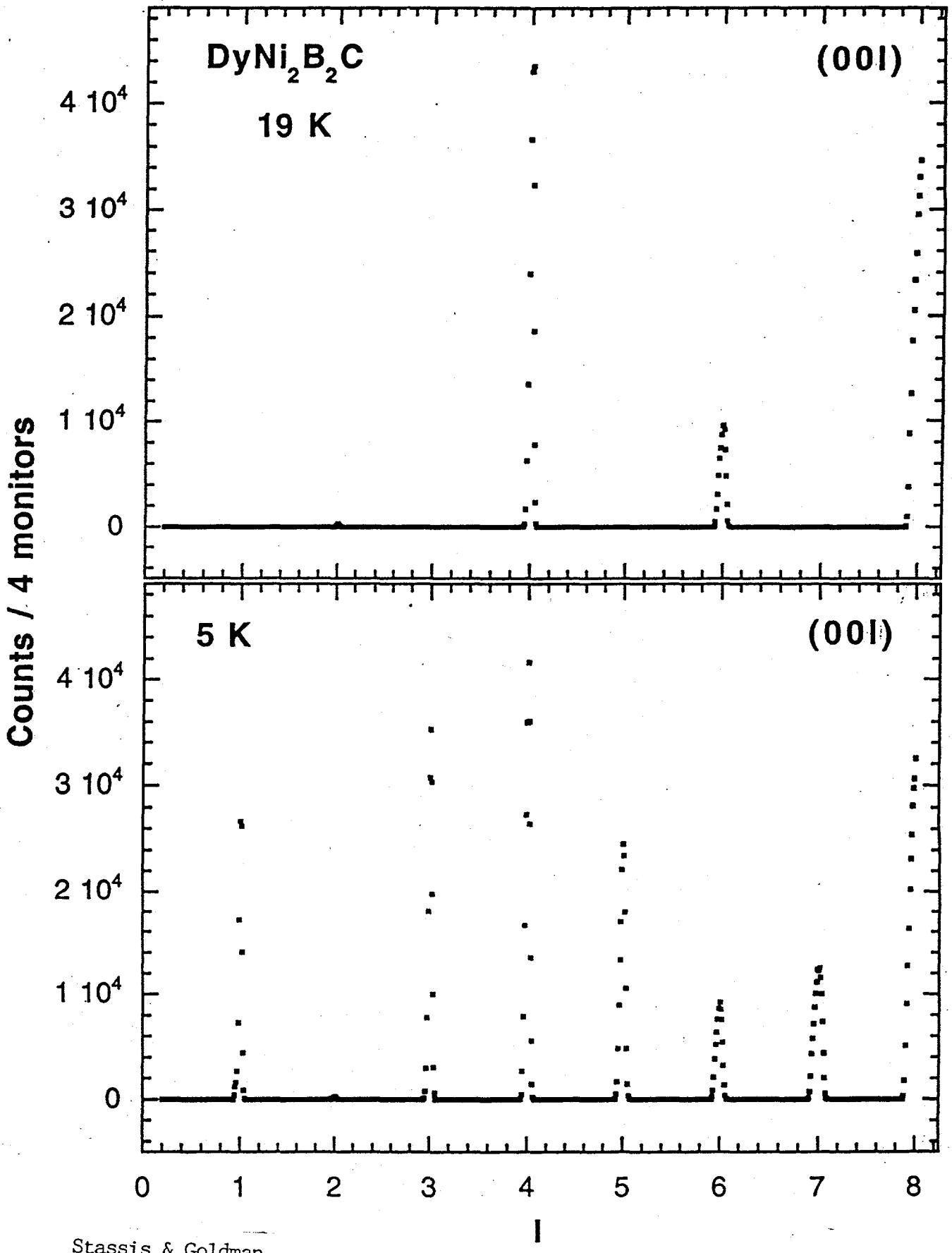

Stassis & Goldman
Fig. 2

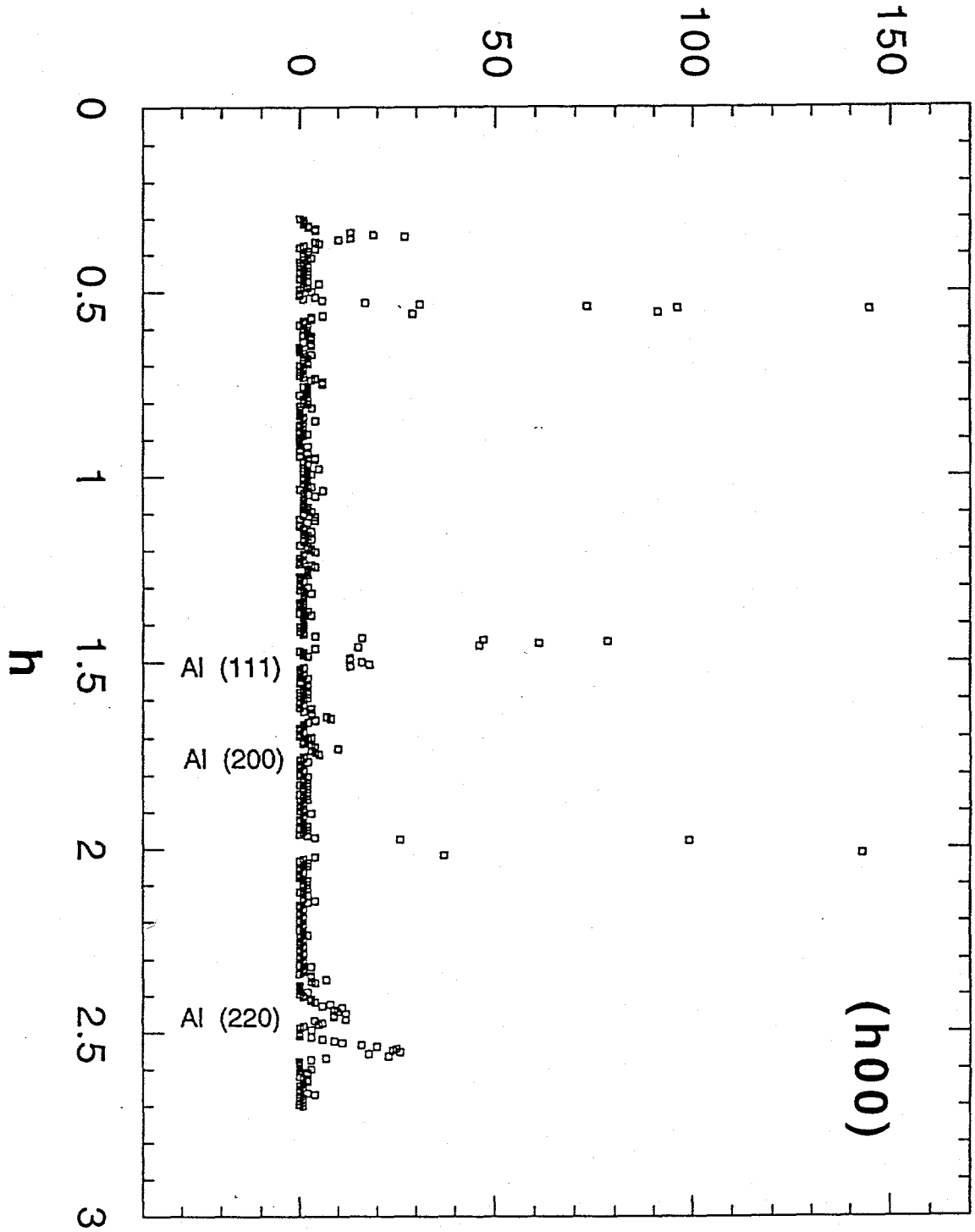

Stassis & Goldman
Fig. 3

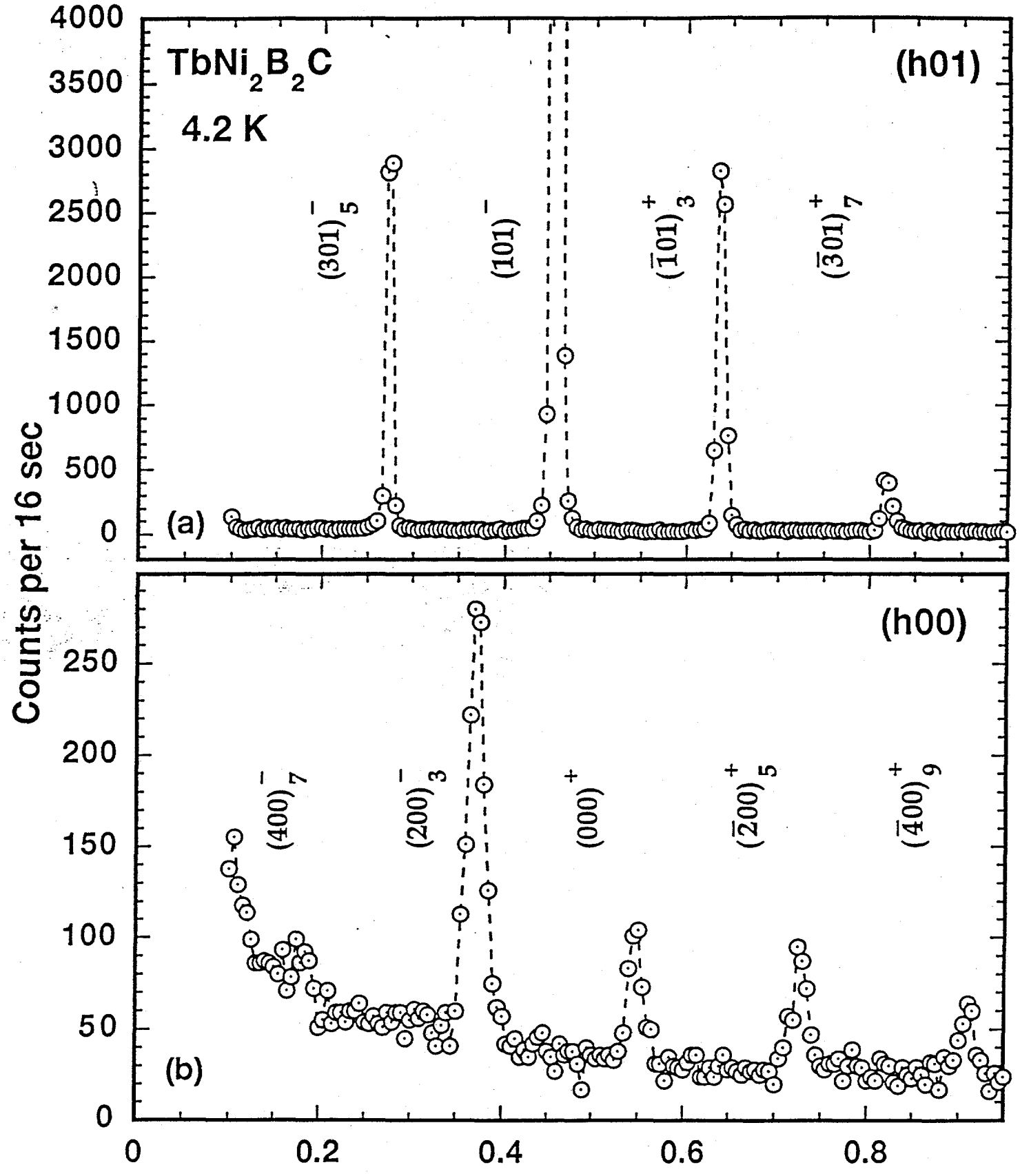

Stassis & Goldman
Fig. 4

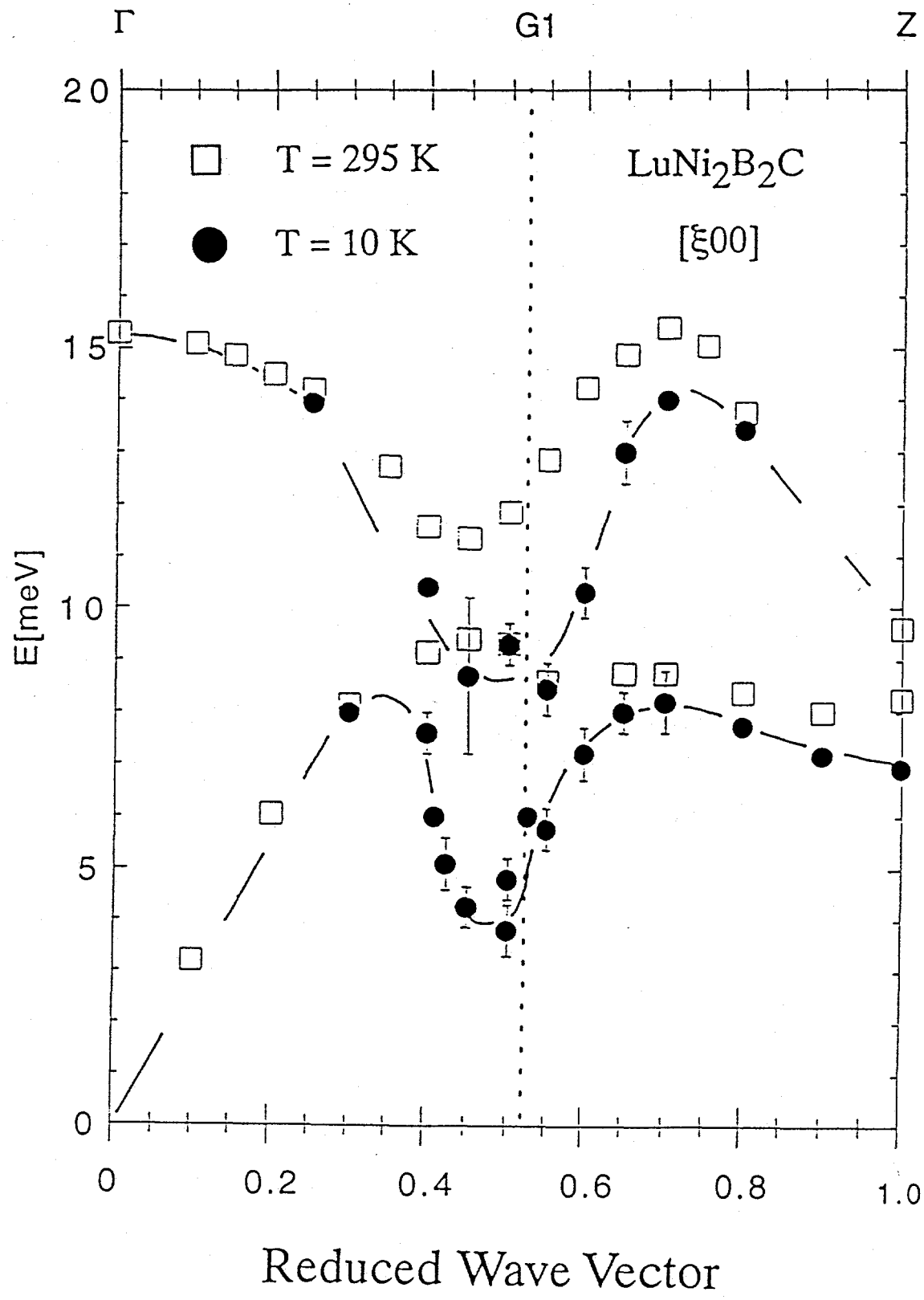

Stassis & Goldman
Fig. 5